Journal of Geodesy (2001) 75: 505–514

Journal of Geodesy

High-resolution gravity field modeling with full variance–covariance matrices

T. Gruber

GeoForschungsZentrum Potsdam, Division 1: Kinematics and Dynamics of the Earth, Telegrafenberg, D-14473 Potsdam, Germany e-mail: gruber@gfz-potsdam.de; Tel.: +49-8153-281578; Fax: +49-8153-281735

Received: 14 August 2000 / Accepted: 7 May 2001

Abstract. High-resolution gravity field models are currently computed by a combined least-squares adjustment with the full variance–covariance matrix for the lower degrees and a simplified approach for the higher degrees. Simplification for the high degrees means that numerical quadrature is applied or that the structure of the covariance matrix is reduced to block diagonals. Both methods have been used for several years to compute high-resolution gravity field models. With recent improvements in algorithms and with the use of parallel computers, the degree and order for full variance–covariance matrices could be increased to 180. Several test solutions combining full and block-diagonal normals were computed and compared to independent data sets. These comparisons were made in order to quantify the impact of reducing the normal structures on the gravity field solution. Results showed that, particularly in the spectral domain (spherical harmonic coefficients), the impact cannot be neglected, while in the space domain (e.g. geoid height grid) the impact is almost negligible.

Key words: Gravity Field – Least Squares

1 Introduction

In view of the future gravity field missions Challenging Minisatellite Payload (CHAMP) (Reigber et al. 1999, 2000), Gravity Recovery and Climate Experiment (GRACE) (Tapley and Reigber 2000) and Gravity Field and Steady-state ocean circulation mission (GOCE) (European Space Agency, ESA 1999), the degree and order of satellite-derived gravity field spherical harmonic series will increase drastically in the future. It is expected that static gravity field solutions, containing the full gravity signal, will be determined up to degree 160 with GRACE (Stanton 2000, p. 18) and up to degree 300 with GOCE (ESA 1999, p. 181). This means that the number of gravity field parameters to be determined by least squares (LS) will increase from 10 000 at present to about 90 000 in the future. Based on the simulations for GRACE and GOCE, which have been performed by several groups (National Research Council, NRC 1997; ESA 1999), it is clear that high-resolution gravity field models (to degree 180 and above) will in future be based to a large extent on satellite information [satellite-to-satellite tracking (SST) data and gradiometer observations from space], while surface gravimetric and altimetric data will only be valuable for the determination of the higher frequencies.

The US–German dual-satellite mission GRACE (Tapley and Reigber 2000), to be launched by the end of 2001 (500-km initial altitude, 89° inclination, 220-km separation, 5 years' duration), will provide SST data in the low–low and high–low modes. The main instruments for gravity field determination are the K-band ranging systems (μm accuracy), the GPS receivers and the accelerometers on board both satellites. Mission goals are the determination of the time-variable and medium-wavelength static gravity field. The ESA mission GOCE (ESA 1999), planned to be launched in 2005 (initial altitude 270 km, inclination 96.5°, two 6-month observation periods with 5 months' interruption), will provide gradiometer data and satellite-to-satellite data in the high–low mode. Acceleration differences between two accelerometers, which are placed some distance apart, are the basic gradiometry observables. By using three pairs of accelerometers, differences in all three spatial directions will be measured. These differences correspond to the second derivatives of the gravitational potential and represent a direct measurement of the gravity field from space (Rummel 1997). The goal of the mission is the determination of the high-resolution static gravity field. The currently flying German CHAMP mission (Reigber et al. 1999, 2000) (initial altitude 454 km, inclination 87°, 5 years' duration) provides high–low SST and accelerometer observations for determination of the long-wavelength gravity field. Therefore, in future, a huge number of continuous gravity field observations will be available. In addition, with the high sensitivity of

GRACE and GOCE, the spatial resolution of satellite gravity fields can be increased significantly.

Continuous observations and increased resolution imply that computational requirements on the data processing will increase by several magnitudes, if a systematic processing of gravity field data is to be performed. To quantify this: the computer time for setting up normal equations for a single gravity anomaly observation increases by a factor of four if we increase the spherical harmonic series degree from 120 to 180. Further on, with the continuous and multi-satellite measurements, the number of observations also increases by several magnitudes with respect to current satellite tracking systems. The computational requirements will be partly fulfilled in future by using faster computer processors and with the development of parallel processing strategies, and partly by the development of more efficient algorithms for setting up the normal equations, as was described by for example, Kim and Tapley (2000). However, methods for reducing computational requirements also have to be investigated by taking advantage of regular matrix structures. Such regular block-diagonal structures can be reached under certain conditions with surface gravity data (Colombo 1981) and also with satellite gradiometer data, if small correlations are neglected (CIGAR III, 1995).

The following sections of this paper deal with two specific problems in the frame of solving large linear systems and reduced normal matrix structures: (1) investigation of the solution strategy for large gravity field normal equation systems up to degree 180 with full variance–covariance matrix on parallel computers and (2) investigations of reduced block-diagonal normal equation systems versus full systems and their influence on the resulting gravity field.

2 Degree 180 gravity field solution

2.1 Set-up of normals up to degree 180 (GRIM5 test case)

Recently, new satellite-only (GRIM5-S1 up to degree 99 and order 95) and combined (GRIM5-C1 up to degree and order 120) gravity field models have been computed by a German–French cooperation between GFZ Potsdam and GRGS Toulouse (Biancale et al. 2000; Gruber et al. 2000b). Based on these experiences the resolution of the combined gravity field model was extended to degree and order 180 using the same data sets as for GRIM5-C1. These are as follows:

(1) NIMA $30' \times 30'$ terrestrial and airborne mean gravity anomalies including standard deviations and topographic heights (Lemoine et al. 1998).
(2) NIMA $1° \times 1°$ mean terrestrial and ship gravity anomalies including standard deviations and topographic heights (Lemoine et al. 1998).
(3) NIMA $30' \times 30'$ mean altimetric and sea-ice gravity anomalies including standard deviations (Lemoine et al. 1998).
(4) $1° \times 1°$ mean gravity anomalies computed from the GRIM5-S1 model for areas not covered by the above data sets (approximately 10% of the Earth's surface).

Each data set was prepared such that gravity field normal equations could be computed and combined with the satellite-only normals. Gravity anomalies were corrected for the ellipsoidal effect on the spherical definition of gravity anomalies and transformed to the GRIM5-S1 reference ellipsoid. In order to reduce the number of observations, $1° \times 1°$ block means corresponding to degree and order 180 of a spherical harmonic series were computed from the original data by applying a mean value operator. In this way, the number of operations for setting up the normal equations could be reduced by a factor of 4. To avoid leakage of higher frequencies into the gravity field solutions, a low-pass filter was applied prior to the spherical harmonic analysis, which removes frequencies above degree 180 (Gruber et al. 2000a). The filter is designed in the following way. (1) The input data set is analyzed by numerical quadrature up to degree and order 360. (2) Residual gravity anomalies are computed from all coefficients above degree 180 (degree 181–360). (3) The resulting residual gravity anomalies are subtracted from the input data set before they are used for gravity field determination. Overlapping ship gravimetry blocks along coastlines (5-degree coast mask) were included to stabilize the altimetry–gravimetry boundary value problem. The altimetry–gravimetry boundary value problem is defined as the determination of a geopotential surface from gravity measurements (gravimetry) over land and geoid height measurements (altimetry) over the oceans. Because altimetric gravity anomalies are derived from altimetric geoid gradients, the combination with measured gravity can also be regarded as an altimetry–gravimetry boundary value problem. This problem has not been solved theoretically to date, but can be overcome by using the LS estimation technique. However, along the boundaries (coastlines), uncertainties are introduced due to the different sources of gravity information. The overlapping method of altimetric and gravimetric derived information is used in order to try to minimize this kind of error. Gravity anomalies standard deviations were prepared in the same way as for GRIM5-C1. For land gravimetry data standard deviations were set in the range between 1.6 and 5.6 mGal, for altimeter-derived gravity anomalies between 1.0 and 3.8 mGal, and for ship gravimetry between 5.0 and 15.0 mGal. Standard deviations of fill-in gravity anomalies from the GRIM5-S1 model were set to a fixed value of 3.2 mGal.

For each $1° \times 1°$ block, mean-value full normal equations up to degree 180 with individual weighting from the prepared standard deviations were set up. Computational requirements for normal equation computation are quite large. The number of spherical harmonic gravity field coefficients is 32 761. Taking into account normal matrix symmetries, the file size of the normal equations becomes about 4.3 Gb if all elements are stored as 8-byte real numbers. There are two options for designing the software. First, the normal matrix is held not in the core but on a hard disk and the matrix is updated step by step, always reading and writing the matrix file. Second, the normal matrix is held in the computer memory all the time and written once at the end of the job. Both methods have advantages and disadvantages, which can be summarized as follows.

(1) The out-of-core method requires high-performance input–output operations.
(2) The out-of-core method enables easy parallel processing by setting up normals for different sub-areas of the data set, if enough disk space is available. For final solution, normals are added afterwards. Relative weighting of normal equation sets can be done during addition.
(3) The in-core method requires large computer memory.
(4) The in-core method enables parallel processing by setting up normals for observations in parallel and updating the normal matrix step by step. For this, tools for sequencing the normal matrix update have to be implemented (e.g. the message-passing interface library, MPI).

Taking into account the existing software and available computers, it was decided to apply the out-of-core method for normal generation. For the computations a SUN Enterprise 450 with 4 Gb memory, four processors with 400 MHz each and enough disk space was used. For computing the normal equations for 1 block, a mean value of about 100 s computer time is necessary, which equates to 1800 CPU hours (or 75 CPU days) for 64 800 data points in the case of global coverage. By using of all four processors the computation time could be reduced to 450 hours (or about 19 days). Because this job is done only once, computational resources are adequate. If we consider GRACE and GOCE satellite data processing of 5-s-apart range or gradiometry measurements (17 280 observations per day), we need about 480 CPU hours per day, if we assume that the computation time and computer are the same as for the above case. Using additionally the high–low GPS SST data, computational requirements show significant further increase. This clearly shows that satellite data processing will be a real challenge for science data systems and that new approaches for the development of faster algorithms and parallelization are necessary.

After combination of all gravimetric, altimetric and fill-in normal equation systems the GRIM5-S1 normals without the Kaula regularization were added. No separate weighting of individual normal equations was applied during addition. This means that it is assumed that the relative weights for all the data sets are correct. Further on, well-determined GRIM5-S1 low-degree and low-order satellite model coefficients were selected to be used as quasi constraints in the combined system. For these coefficients a diagonal normal equation system with weights taken from the coefficients' standard deviations was generated and added to the overall system (Gruber et al. 2000b). After this point the normal equation system for the 180° gravity field model was complete.

2.2 *Large linear system solver*

As mentioned above, a normal equation system of 4.3 Gb size (after removal of symmetric elements) has to be inverted and solved, such that the complete variance–covariance matrix is available. Because of the huge size, standard single-processor inversion algorithms are no longer adequate for this problem. Therefore, parallelized algorithms have to applied. There are several standard libraries available, such as LAPACK (Anderson et al. 1999) or PLAPACK (van den Geijn 1997), which can solve such problems. For our purposes the SUN Performance Library 3.0 included in the early access version of SUN Workshop 6 was used. This library is based on the BLAS, LINPACK, LAPACK and some other libraries and supports 64-bit code, which is necessary for addressing the matrix elements. Generally, there exist two strategies to solve such large linear systems, depending on the computer architecture. These are as follows.

(1) Distributed-memory multi-processor machines: each processor has a fixed size memory. By combining several processors large systems can be solved. For communication between processors the message-passing interface library (MPI) has to be used.
(2) Shared-memory multi-processor machines: each processor can use the full memory. No MPI has to be used for communication.

The source code has to be adapted to the machine architecture, such that optimized computation times can be reached. As before, a SUN Enterprise 450 shared-memory machine was used to compute the solution. Three LAPACK subroutines included in the SUN performance library were used to perform Cholesky decomposition, computation of the inverse of the triangular matrix and matrix multiplication. A drawback of all standard libraries is that symmetric matrices with reduced storage requirements cannot be handled. This means, in our case, that the full symmetric matrix of about 8.6 Gb size has to be stored. This is more than double the available computer memory of 4 Gb. Therefore, additional swap space on a local hard disk was assigned in order to be able to hold the full matrix. The solution, including reading the matrix and writing the variance–covariance matrix, required about 10 hours of user time on the SUN Enterprise 450. For testing the performance degradation due to the additional large swap space, the same solution was computed on a SUN Enterprise 3500 with 8 CPUs (336 MHz each) and 8 Gb memory. On this machine only a small additional swap space had to be assigned. The solution required, including all reading and writing operations, about 3.5 hours of user time. About 60% of the computer time reduction can be assigned to the larger number of CPUs, while the rest is due to the larger memory. Summarizing, it can be stated that by use of parallel libraries, even on medium-size multi-processor workstations, large linear systems with full variance–covariance matrices can be solved relatively easily.

2.3 *Gravity field quality analysis*

A degree and order 180 solution using identical data as for the GRIM5-C1 model (Gruber et al. 2000b) was computed. In order to quantify the quality of this model some standard tests were performed. As standard tests, orbital fits for the long wavelengths and geoid height comparisons for the full spectrum are usually performed. Table 1 gives an overview of orbital residuals for some low-orbiting satellites using the new GRIM5-C1-180 model compared to GRIM5-S1 (Biancale et al. 2000) and EGM96 (Lemoine et al. 1998). All models are truncated at degree and order 120, because these satellites have no sensitivity to higher degrees. Comparing the numbers for GRIM5-S1 and the new GRIM5-C1-180 models, it can be seen that, except for GFZ-1, no degradation of orbital fits due to inclusion of surface normals occured. This means that long wavelengths are properly modeled. For GFZ-1 an inexplicable degradation is visible. The GFZ-1 satellite is highly sensitive to some resonant orders of the gravity field series. By inclusion of surface data these coefficients could change significantly and could cause the increase of the RMS of orbital fits. In comparison to EGM96, improvements for nearly all satellites are apparent. However, also for the EGM96 model, a relatively large RMS for GFZ-1 is visible, which is mainly caused by the few GFZ-1 observations included in the model. This may be a hint as to the problems in some of the coefficients for the GFZ-1 resonant orders, as for the GRIM5-C1-180 solution.

Table 2 shows statistics of pointwise geoid height differences between the GRIM5-C1-180 and the EGM96 model, which is truncated at degree 180. Numbers show, for all data sets, slightly better results for EGM96 than for the GRIM5-C1-180 model (1–2 cm in RMS). This means that for higher degrees the EGM96 model has more signal. This also is visible in the degree variances of both models (not shown here). The larger signal could be caused by the two-step procedure for determination of these coefficients in the EGM96 model (first: numerical quadrature; second: block-diagonal LS for remaining residuals). For the GRIM5-C1-180 model, all coefficients were determined by a one-step LS estimation.

Table 1. Orbital fits

Satellite (arcs, type)	GRIM5-S1	GRIM5-C1-180	EGM96
Ajisai (4, L)[a]	7.5	7.4	7.6
ERS-1 (9, L)	7.2	7.2	8.3
(9, X)[b]	8.79	8.75	10.35
Starlette (5, L)	8.2	8.3	7.9
GFZ-1 (5, L)	22.4	28.5	47.2

[a] L = Laser (cm)
[b] X = Altimeter crossover (cm)

Table 2. RMS of differences between GPS/leveling-derived geoid heights and model-derived geoid heights (m)

Area (no. points)	GRIM5-C1-180	EGM96
Europe, north–south (67)	0.447	0.430
USA (5168)	0.632	0.614
Canada (1587)	0.510	0.507
Germany, south–west (125)	0.664	0.652
Germany north (42)	0.252	0.232
Uruguay (16)	0.592	0.578

3 Block-diagonal versus full normal matrices

One way to reduce computational efforts during normal equation computation is by the use of regular matrix structures, if possible. In gravity field determination, there are two cases for which reduced normal equation structures are possible.

(1) For surface gravity and geoid data the normal matrix becomes block diagonal if the following conditions are fulfilled (Colombo 1981).
  - Data on a regular grid with equator symmetry and equal angular meridians.
  - Uniform data type with global coverage (e.g. no mix of geoid heights and gravity anomalies).
  - Longitude independent and equator symmetric weighting of data.
  - Parameter vector is sorted first with respect to increasing order and second with respect to increasing degree per order.

(2) For gravity gradiometer data the normal matrix becomes block diagonal if the following assumptions are made (CIGAR III 1995).
  - Continuous gradiometer observations.
  - Equator symmetry of gradiometer data.
  - Parameter vector is sorted first with respect to increasing order and second with respect to increasing degree per order.
  - Neglecting small correlations between gravity coefficients.

It has to be noted that, in the case of gradiometry, the block-diagonal structure cannot be generated strongly by applying specific data rules as for the surface data. Small off-diagonal correlations have to be neglected in order to obtain a block-diagonal system. The goal of this investigation is not to quantify the error made by neglecting some correlations, but simply to show, through experiences with surface gravity data, what the implications are for gradiometer data processing. Therefore, all computations and follow-on investigations are based on surface gravity anomaly data sets. However, it should be kept in mind that gradiometry could be similar to this test case.

3.1 *Test scenario*

In order to test the implication of full versus block-diagonal normal equation systems on the resulting gravity field solution, combinations of different normal equation systems (full and/or block diagonal) were formed and solved for a gravity field. Data and data preparation procedures were the same as described in Sect. 2.1. From the 1° × 1° data sets over land, oceans, and for the remaining gaps, a global data set including standard deviations was generated. From this data set, which was low-pass filtered for degrees above 180 or for degrees above 120 for a second test case, the following normal equation systems were computed.

(1) F180: full system up to degree 180 with individual weighting of data.
(2) F120: full system up to degree 120 with individual weighting of data.
(3) BD180: block diagonal system up to degree 180 with constant weighting.
(4) BD120: block diagonal system up to degree 120 with constant weighting.

In case of the block-diagonal system, the constant weighting factor was computed by the mean of all individual standard deviations. These normal equations then were combined differently with the GRIM5-S1 satellite-only system (G5-S1) and the diagonal system for the low-degree satellite coefficients (G5-S1-D) (see Sect. 2.1). In total, seven different solutions with different combinations were computed; these are summarized in Table 3. Figure 1 shows graphically the combination schemes for all the test models.

Remarks on the test solutions are as follows.

A-180: degree 180 solution with full variance covariance matrix and GRIM5-S1 normal equation systems.

B-180: degree 180 solution composed of full variance covariance solution up to degree 120 combined with GRIM5-S1 normal equations and block-diagonal solution for degree 121 to 180. Correlations for coefficients of high degree (≥121) with low-degree coefficients (≤120) of the same order are neglected.

C-180: same as B-180 except that for high-degree block-diagonal solution all correlations are taken into account. Low-degree coefficients are identical to the B-180 model.

A-120: degree 120 solution with full variance–covariance matrix and GRIM5-S1 normal equation systems.

B-120: degree 120 solution with block-diagonal variance–covariance matrix and GRIM5-S1 normal equation systems.

C-120: degree 120 solution with full variance–covariance matrix and GRIM5-S1 low-degree diagonal system.

D-120: degree 120 solution with block-diagonal variance–covariance matrix and GRIM5-S1 low-degree diagonal system.

Comparisons of test models should show the following effects.

(1) A-180 versus B-180/C-180: effect of full versus block-diagonal normals on high-degree coefficients (> 120).

Table 3. Combination scheme of test solutions

Model	F180	F120	BD180	BD120	G5-S1	G5-S1-D
A-180	*				*	*
B-180		*	*		*	*
C-180		*	*		*	*
A-120		*			*	*
B-120				*	*	*
C-120		*				*
D-120				*		*

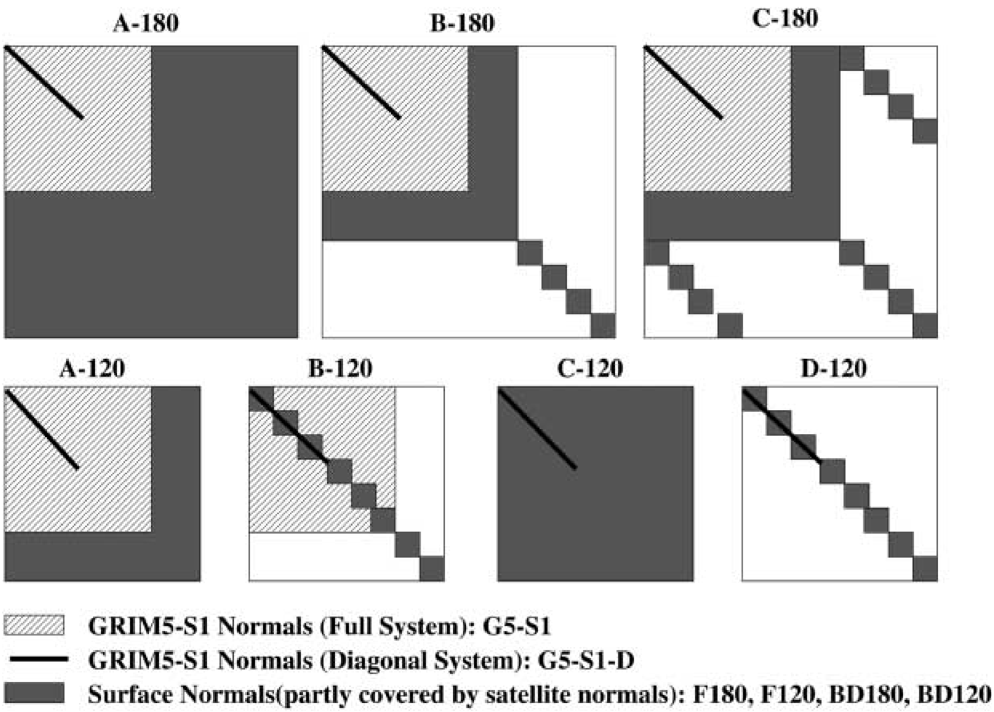

Fig. 1. Normal structures for combination models

(2) B-180 versus C-180: effect of neglecting correlations of high- with low-degree coefficients of same order on high-degree coefficients (> 120).
(3) A-120 versus B-120: effect of full versus block-diagonal normals on low-degree coefficients (≤120) based on full satellite normals.
(4) C-120 versus D-120: effect of full versus block-diagonal normals on low-degree coefficients (≤120) based on low-degree diagonal satellite normals.

3.2 Test results

In order to test the different models, again orbital fit residuals and geoid height comparisons were computed and analyzed (see Sect. 2.3). Table 4 shows the geoid height comparisons for all models with their full resolution of degree and order 120 or 180 respectively.

Figure 2 shows RMS values of differences of geoid height differences (further on called geoid gradient differences) between GPS-derived geoid heights and degree 180 model-derived geoid heights for a small network in south-west Germany. The x-axis shows the distance between the two points, which is mapped to the spherical harmonic degree of the relevant wavelength. For each degree the wavelength is determined by the following: wavelength = 20 000 km/degree. Range classes are separated midway between two wavelengths. All point distances which fall into a specific range class are then used for performing the statistics of gradient differences. By this method, degree-dependent comparisons on the basis of a huge number of differences can be made, because the difference between each GPS point and any other GPS point of the data set is computed. For the south-west German data set with 125 points, we obtain about 3400 gradient differences with about 40 samples per class for degree 100 and above. For lower degrees no samples are available due to the too small distances between GPS points. The rationale for transferring the distances into wavelengths and degrees is to find out if there are any dependencies of the gradient differences from the wavelengths. It should be noted that this transformation can only be regarded as an approximation. Errors in shorter wavelengths are mapped to longer wavelengths for cases when the longer wavelength is a multiple of the shorter wavelength. Nevertheless, this information is valuable for the visualization of possible dependencies between geoid gradient differences and their distances.

Figure 3 shows geoid gradient differences between GPS-derived geoid heights and degree 120 model-derived geoid heights for the Canadian GPS on the benchmark network with 1587 data points in the same domain as in Fig. 2. In this case, several hundred thousand gradient differences are statistically analyzed. Degrees below 50, which are not plotted, show a similar behavior to the higher degrees, with much larger residuals for solutions C and D.

Finally, in order to test the long wavelengths in the spectral domain, orbital fit residuals for the low-degree solutions up to degree 120 are computed and are summarized in Table 5.

3.3 Interpretation of test results

3.3.1 A-180 versus B-180 (effect of full versus block-diagonal normals on high-degree coefficients)

High-degree terms can only be tested by geoid and geoid gradient comparisons with GPS-derived data. Geoid height comparisons (Table 4) do not show a significant difference between the two models. There is no systematic degradation visible when using the reduced block-diagonal normal equation structure. The geoid gradient plot (Fig. 2) shows slightly increased RMS values for the block-diagonal model (△) compared to the full solution (□) over the full spectrum, which is plotted in Fig. 2. Using other GPS data sets, both RMS values are always close together over the full spectrum without dominant larger RMS values for one of the two gravity models. As a consequence of these comparisons, it can be stated that block-diagonal and full normal equation systems provide similar results for the higher frequencies (degree 120 to 180), if they are mapped to geoid heights. In other words, block-diagonal normals are adequate for the estimation of high-degree coefficients.

3.3.2 B-180 versus C-180 (effect of high- with low-degree correlations of same order on high-degree coefficients)

Statistics of model and GPS geoid height differences provide roughly the same results for both models (Table 4). The situation changes if geoid gradient differences are considered (Fig. 2). In Fig. 2 it can be identified that solution C-180 (∇) has significantly larger RMS values for the long wavelengths than solution B-180 (△). For the short wavelengths (> 120), differences become smaller and finally disappear. This test shows that

Table 4. RMS of differences between GPS/leveling-derived geoid heights or altimetry-derived geoid heights and gradients with model-derived geoid heights (m) and gradients (cm/km)

Area	A-180	B-180	C-180	A-120	B-120	C-120	D-120
Europe	0.451	0.445	0.445	0.666	0.673	0.693	0.731
USA	0.632	0.631	0.633	0.780	0.793	0.744	0.751
Canada	0.511	0.510	0.513	0.651	0.666	1.293	1.259
Germany, south–west	0.664	0.660	0.653	0.742	0.733	0.755	0.755
Germany, north	0.252	0.260	0.274	0.290	0.303	0.318	0.307
Uruguay	0.590	0.565	0.576	0.677	0.663	0.675	0.687
Altimetric height	0.742	0.741	0.742	0.848	0.867	0.842	0.851
Altimetric gradient	1.724	1.726	1.726	1.765	1.769	1.763	1.766

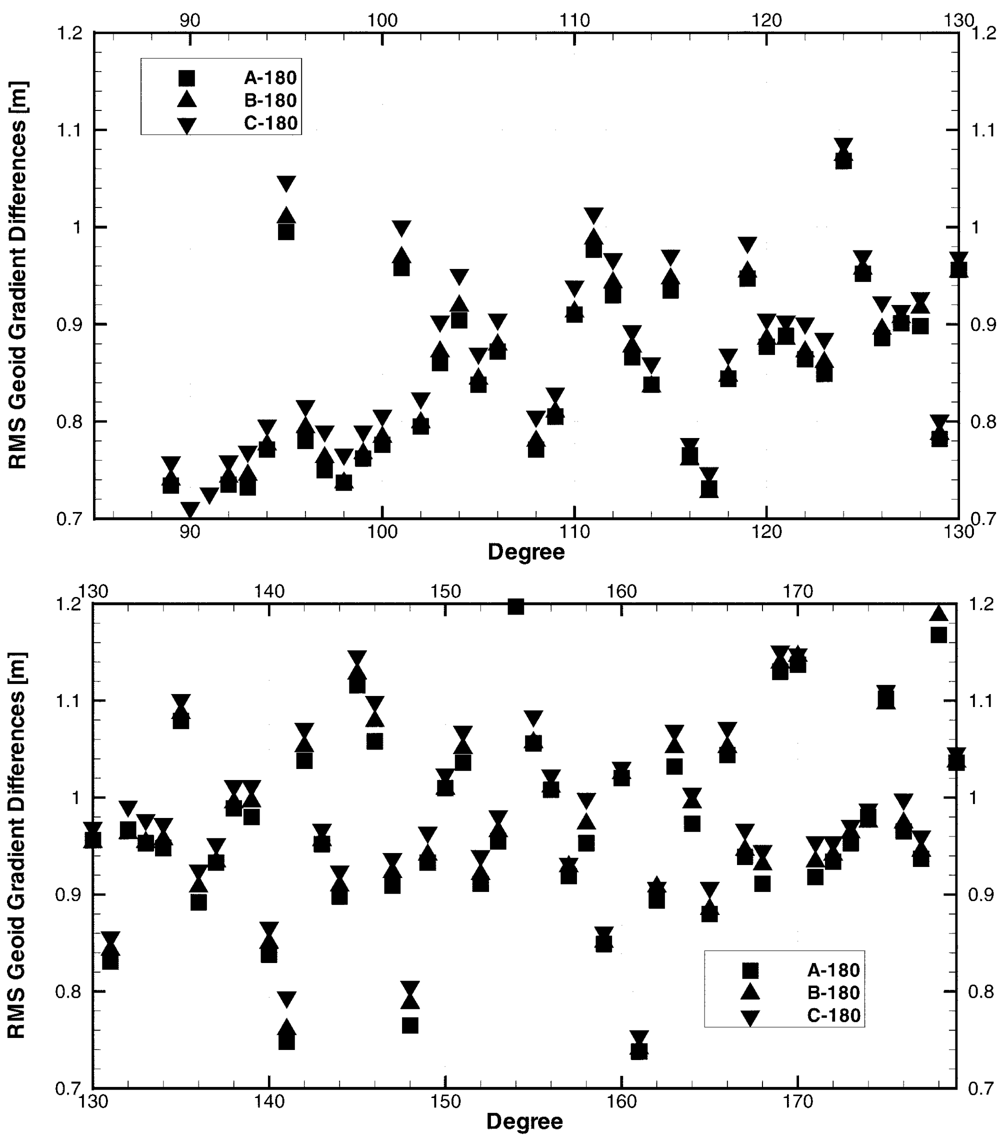

Fig. 2. RMS of geoid gradient differences for the south-west German GPS geoid height data set with respect to degree (m)

neglecting the correlation of high- with low-degree coefficients has positive effects for the long-wavelength geoid gradients. The reason is that for the test case low- and high-degree coefficients are mixed and are not estimated in a common LS solution. Coefficients from both solutions do not entirely fit together, therefore neglecting correlations provides better results for the test case. The situation changes when also low-degree coefficients are estimated in a single LS process with all correlations, as was done for another test solution. Then, the RMS values for all test data sets are close to solution B-180 or even better. For the high-degree terms only small differences in RMS values are visible. For some other GPS networks high-degree RMS values for solution B-180 are even slightly larger than for C-180. Overall, results show only small differences between the two models for the high-degree terms. The following conclusion can be drawn from this test case. If correlations should be taken into account, a one-step LS approach, combining full and block-diagonal normals, for the complete spherical harmonic series, should be used. If a two-step LS procedure is used (full system solution for low degrees, block-diagonal solution for high degrees), correlations for high-degree terms should be neglected, because they could cause additional long-wavelength problems in the geoid.

3.3.3 A-120 versus B-120 (effect of full versus block-diagonal normals on low-degree coefficients)

Both models are based on the full GRIM5-S1 satellite-only normal equation system and the low-degree GRIM5-S1 diagonal system. They differ only by the normal equation structure for the surface data. Several tests are performed with these models. Geoid height difference statistics at GPS stations (Table 4) show for most data sets a slight increase in RMS values when using the block-diagonal structure. This indicates a small degradation of geoid height accuracy. Similar results are visible when looking at the geoid gradient differences on GPS stations (Fig. 3). The Canadian data set clearly shows an increase of RMS values for the full spectrum (□ versus △). This is also true for all other available test data sets. As an additional test for the long

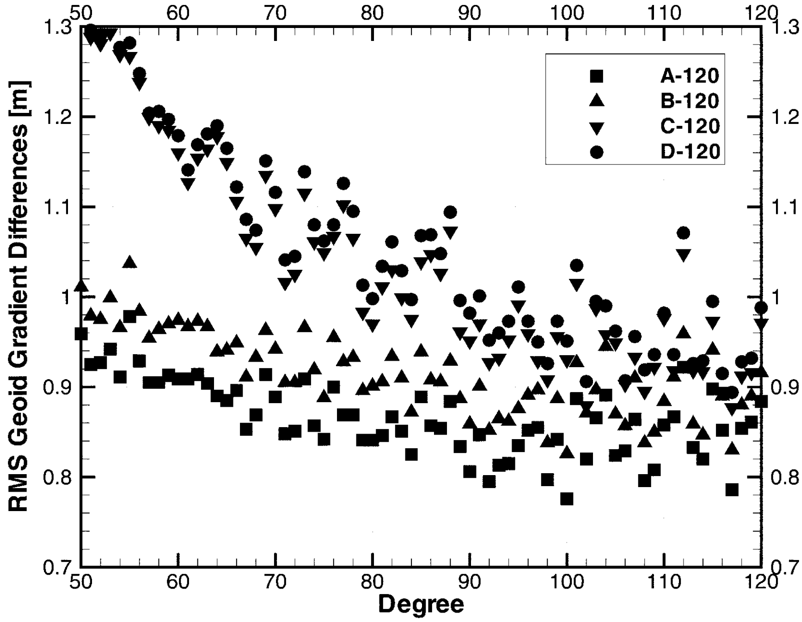

Fig. 3. RMS of geoid gradient differences for the Canadian GPS geoid height data set with respect to degree (m)

wavelengths, orbital fit residuals are computed (Table 5). In Table 5, only small differences are visible between the A-120 and the B-120 model. While for Starlette a small decrease in the RMS value appears, for GFZ-1 an increase is visible. This could be a hint as to the poorer quality of the B-120 model, because GFZ-1 is more sensitive to higher degrees, which are mainly determined from surface data. In summary, these tests indicate a poorer gravity field quality for block-diagonal models, when mapped to the geoid, and some problems in the spectral domain (spherical harmonic representation), which are overlaid by the good performance of the satellite-only model.

3.3.4 C-120 versus D-120 (effect of full versus block-diagonal normals on low-degree coefficients)

In order to determine the influence of the satellite-only normal equations on the long wavelength test results, alternative solutions with full (C-120) and block-diagonal (D-120) surface normal equations are computed, which are based only on the very-long-wavelength satellite-derived coefficients, introduced as a diagonal normal equation system. In this case the effect of full versus block-diagonal surface normals should be better visible than before. From the geoid height comparisons on GPS stations (Table 4), it cannot be identified which of the two models performs better. From the altimeter comparisons, model D-120 shows a small degradation with respect to C-120, which is not very significant. Comparing these solutions with A-120 and B-120, in some cases better results appear, if not the full satellite-only normal matrix is used. This shows that this single type of test cannot be regarded as a quality criterion for a gravity field model. When looking at the geoid gradient RMS values for the Canadian data set (Fig. 3), it can be clearly seen that C-120 and D-120 are significantly above A-120 and B-120. In particular the long wavelengths are much more poorly determined (RMS values below degree 50 are further increased). Comparing C-120 (∇) and D-120 (○), it can be seen that the block-diagonal solution (D-120) is generally above the full variance–covariance solution (C-120). This is an indicator that reduced normal equation structures also imply reduced geoid quality in the space domain. In order to test the spectral domain, again orbital fit residuals are computed (Table 5). Because of not using the full satellite-only normal equation system, RMS values are significantly increased for this test. It can also be seen that for all satellites the block-diagonal model (D-120) has larger RMS values than the model with full surface normals (C-120). Now, in contrast to the previous case, a clear degradation in the spectral domain can be identified if block-diagonal surface normals are used instead of full normal equation systems.

Table 5. Orbital fits

Satellite (arcs, type)	A-120	B-120	C-120	D-120
Ajisai (4, L)[a]	7.38	7.38	57.4	58.3
ERS-1 (9, L)	7.19	7.19	114.0	148.5
(9, X)[b]	8.75	8.75	95.8	117.3
Starlette (5, L)	8.27	8.22	99.9	105.5
GFZ-1 (5, L)	24.49	29.02	164.3	188.8

[a] L = Laser (cm)
[b] X = Altimeter crossover (cm)

4 Summary and conclusions

Two specific problems in the frame of high-resolution gravity-field modeling with LS have been investigated: (1) the set-up and solution of large gravity field normal equation systems; and (2) the, influence of reduced block-diagonal normal equation structure compared to full variance–covariance matrices on gravity field models.

Experiences gained during the GRIM5-C1 gravity field model computation have been used to set up normal equation systems from altimetry and gravimetry data up to degree and order 180. In order to run several processes in parallel, an out-of-core method was used for computation. This means that computer memory requirements are small, while disk space and input/output requirements are high. On average, 100 s CPU time on a medium-class workstation are required per surface observation. In the case of a limited surface data set this is a manageable task, while in the case of satellite-to-satellite tracking data with a huge amount of daily data points, new approaches and algorithms have to be developed. The LS solution of the normals can be performed relatively easily by using standard parallel libraries. On multi-processor workstations, depending on the number of available processors and memory, between 3.5 and 10 hours of user time were necessary to perform Cholesky decomposition and triangular matrix inversion. Using these algorithms an extended GRIM5-C1 model, complete to degree and order 180, was computed and compared to GRIM5-S1 for the long wavelengths and to EGM96 for the full spectrum. Results show that for the long wavelengths the new GRIM5-C1 180 model performs better than EGM96, while for the higher degrees, corresponding to short wavelengths, EGM96 has more signal and consequently smaller differences to point geoid heights. Generally, it could be proved that high-resolution combined gravity field models to degree and order 180 can be computed with available resources relatively easily and with numerical stability.

In the second part of the present paper the influence of reduced block-diagonal normals compared to full normal equation systems on combined gravity field models was investigated. This question is important, because computational efforts could be reduced drastically and the resolution of gravity field models could be increased to 360, and even more, if block diagonals are adequate. Further on, this question could be relevant for data processing of the GOCE gradiometry data with quasi block-diagonal normal equation structures. Tests were performed on the basis of the GRIM5-C1 data and the derived normal equations. Seven solutions with different degrees and different combinations of full and/or block-diagonal normals were computed. All solutions were tested with independent geoid heights on GPS stations (heights and gradients) as well as orbital fit residuals. From these tests the following conclusions can be made.

(1) Geoid height and gradient tests show a small degradation for block-diagonal models for short wavelengths when compared to full variance–covariance solutions.
(2) Mixing coefficients from full and block-diagonal solutions is not adequate, if correlations between low- and high-degree coefficients for the same order are used in a different way for both solutions.
(3) For long wavelengths, a degradation for block-diagonal models is visible in orbital fit residuals, if the normal equation system is not dominated by the satellite-only normals.
(4) Geoid gradient comparisons show a degradation for block-diagonal models. Geoid height comparisons are not influenced significantly by normal equation structure.

Summarizing, it can be stated that block-diagonal solutions are slightly worse than solutions based on full variance–covariance matrices. This is especially visible in the spectral domain, while in the space domain (e.g. geoid heights) it is difficult to quantify. This indicates that errors in the spherical harmonic coefficients (spectral domain), which are caused by reduced normal structures, are in summary not mapped back to the geoid (space domain). For a consistent gravity field estimation, full normal equation systems should be used as much as possible. Higher-degree terms, which exceed the computational resources, can be determined with the block-diagonal technique relatively accurately, if we consider them in the space domain.

References

Anderson E, Bai Z, Bischof C, Demmel J, Dongarra J, Du Croz J, Greenbaum A, Hammaarling S, McKenney A, Ostrouchov S, Sorensen D (1999) LAPACK users guide, 3rd edn. Society for Industrial and Applied Mathematics, Philadelphia

Biancale R, Balmino G, Lemoine JM, Marty J-M, Moynot B, Barlier F, Exertier P, Laurin O, Gegout P, Schwintzer P, Reigber Ch, Bode A, König R, Massmann F-H, Raimondo JC, Schmidt R, Zhu S (2000) A new global earth's gravity field model from orbit perturbations: GRIM5-S1. Geophy Res Lett 27 (22): 3611–3614

CIGAR III (1995) Study on precise gravity field using gradiometry and GPS. Phase final report, ESA-contract 10713/93/f/FL

Colombo O (1981) Numerical methods for harmonic analysis on the sphere. Rep 310, Department of Geodetic Science and Surveying. The Ohio State University, Columbus

European Space Agency (1999) Gravity Field and Steady-State Ocean Circulation Mission (GOCE). Report for mission selection – the four candidate Earth explorer core missions: SP-1233(1)

Gruber Th, Reigber Ch, Schwintzer P (2000a) The 1999 GFZ pre-CHAMP high resolution gravity model. In: Schwarz KP (ed) Proc IAG Symp, vol 121, Geodesy beyond 2000, IAG General Assembly, Birmingham, 1999. Springer, Berlin Heidelberg New York, pp 89–95

Gruber Th, Bode A, Reigber Ch, Schwintzer P, Balmino G, Biancale R, Lemoine J-M (2000b) GRIM5-C1: combination solution of the global gravity field to degree and order 120. Geophys Res Lett 27 (24): 4005–4008

Kim MC, Tapley BD (2000) Formation of surface spherical harmonic normal matrices and application to high-degree geopotential modeling. J Geod 74: 359–375

Lemoine FG, Kenyon SC, Factor JK, Trimmer RG, Pavlis NK, Chinn DS, Cox CM, Klosko SM, Luthcke SB, Torrence MH, Wang YM, Williamson RG, Pavlis EC, Rapp RH, Olson TR (1998) The development of the joint NASA GSFC and National Imagery and Mapping Agency (NIMA) geopotential model EGM96. NASA Tech Paper NASA/TP-1998-206861, Goddard Space Flight Center, Greenbelt, MD

National Research Council (1997) Satellite gravity and the geosphere. National Academic Press, Washington, DC

Pavlis NK, Chan JC, Lerch FJ (1996) Alternative estimation techniques for global high-degree gravity modeling. In: Rapp, Cazenare, Nerem (eds) Proc IAG Symp 116, Global gravity field and its temporal variations. Springer, Berlin Heidelberg New York, pp 111–120

Reigber Ch (1989) Gravity field recovery from satellite tracking data. In: Sansò F, Rummel R (eds) Lecture notes in Earth sciences 25. Springer, Berlin Heidelberg New York

Reigber Ch, Lühr H, Schwintzer P (1999) The CHAMP geopotential mission. Boll Geofis Teor Appl, Special Section for Joint IGC/IgeC symp, Trieste, 1998, Vol.40–N.3–4, p. 277–284

Reigber Ch, Lühr H, Schwintzer P (2000) CHAMP mission status and perspectives. EOS Trans AGU 81(48) (Suppl)

Rummel R (1997) Spherical spectral properties of the Earth's gravitational potential and its first and second derivatives. Lecture notes in Earth sciences 65. Springer, Berlin Heidelberg New York

Stanton R (2000) GRACE science and mission requirements document (327–200), rev. C, 16 August 2000; document JPL D-15928, NASA Jet Propulsion Laboratory, Pasedena

Tapley BD, Reigber Ch (2000) The GRACE mission: status and future plans. EOS Trans AGU 81(48) (Suppl)

van de Geijn (1997) Using PLAPACK. Scientific and Engineering Computation Series, MIT Press, Cambridge, MA